Volume 16
Number 7
21 February 2025
Pages 2937–3348

Chemical Science

rsc.li/chemical-science

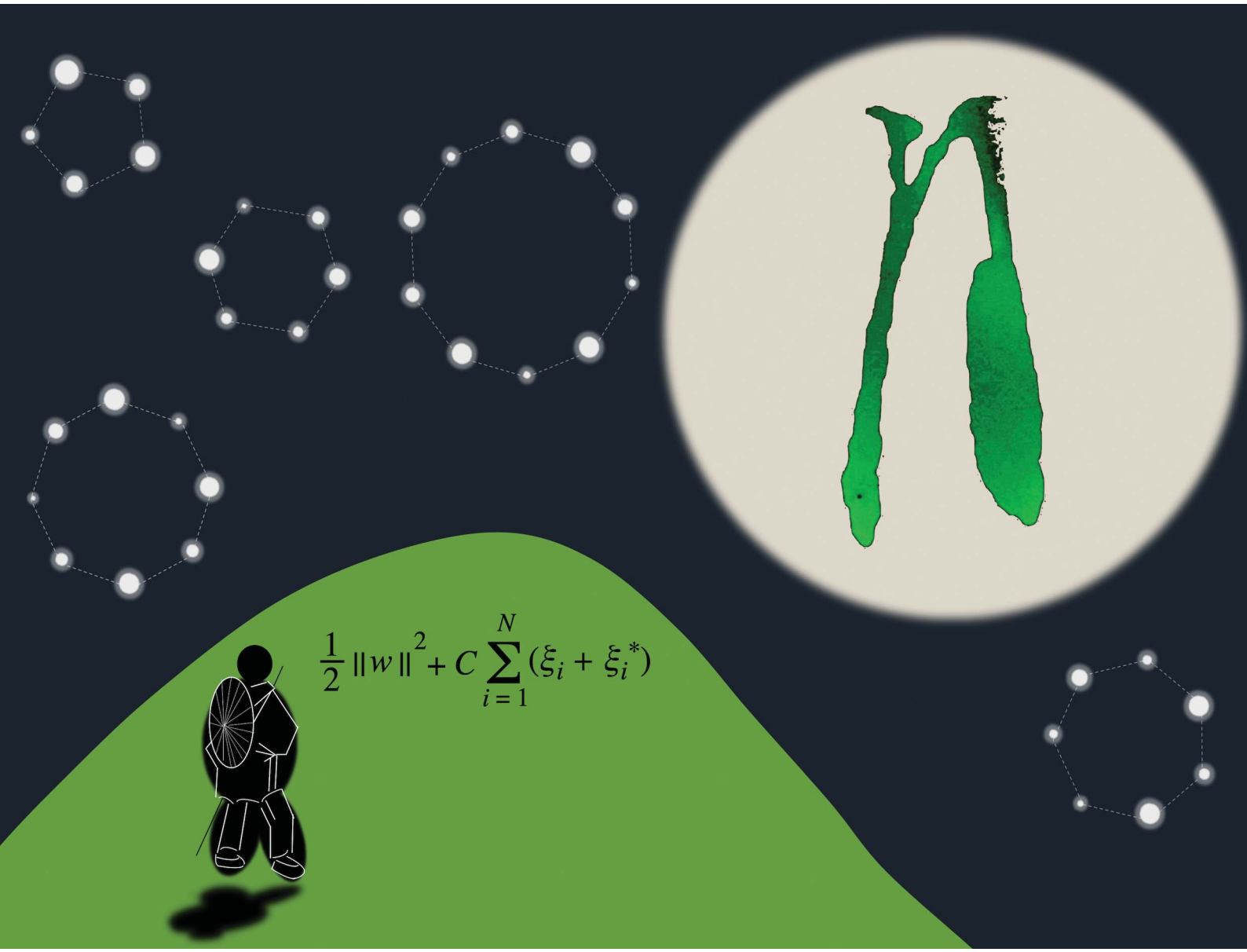

ISSN 2041-6539

ROYAL SOCIETY OF CHEMISTRY

EDGE ARTICLE
Koki Ikemoto, Hiroyuki Isobe *et al.*
Optimising reaction conditions in flasks for performances in organic light-emitting devices

15 YEARS ANNIVERSARY

Chemical Science

ROYAL SOCIETY OF CHEMISTRY

EDGE ARTICLE

View Article Online
View Journal | View Issue

Cite this: *Chem. Sci.*, 2025, **16**, 3045

All publication charges for this article have been paid for by the Royal Society of Chemistry

Received 16th October 2024
Accepted 20th December 2024

DOI: 10.1039/d4sc07039a

rsc.li/chemical-science

Optimising reaction conditions in flasks for performances in organic light-emitting devices†

Koki Ikemoto, ‡*[a] Misato Akiyoshi,‡[a] Ayano Kobayashi,[a] Hiroshi Kita,[b] Hideo Taka[b] and Hiroyuki Isobe *[a]

A method for correlating reaction conditions with device performance was developed by combining Design-of-Experiments and machine-learning strategies in multistep device fabrication processes. This method allowed the "from-flask-to-device" optimisation of a macrocyclisation reaction yielding a mixture of methylated [*n*]cyclo-*meta*-phenylenes, and a crude raw material was directly applied to the fabrication of Ir-doped organic light-emitting devices *via* spin-coating. The method succeeded in eliminating energy-consuming and waste-producing separation and purification steps during device fabrication. The device using the optimal raw mixture material recorded a high external quantum efficiency of 9.6%, which surpassed the performance of purified materials. The raw material method was also found to be applicable to screen-printing processes, and image-transferred OLEDs were fabricated using the low-cost, environmentally benign materials.

Introduction

Optimising reaction conditions in flasks for high-yield synthesis is a common process that is performed ubiquitously in synthetic laboratories. The most popular method of optimisation is known as one-factor-at-a-time (OFAT) optimisation,[1] where each factor is examined one at a time. The OFAT optimisation is particularly useful for reactions with simple pathways, which can also lead to mechanistic insights.[1,2] For reactions with complicated pathways, however, Design-of-Experiments (DoE) optimisation can often be superior because it more effectively covers the parameter space for optimisation.[3] Recently, we augmented the DoE optimization data with machine-learning (ML) predictions, which allowed us to find an optimal condition for a reaction passing through complicated pathways with a heatmap representation of the yields in the parameter space (Fig. 1).[4] Observing that the "DoE + ML" method was able to correlate the reaction conditions with the yields (outcome of a single experimental process, *i.e.*, reaction) despite the complicated pathways, we came up with the idea of correlating the reaction conditions with the outcome to be derived after multiple experimental processes using the DoE + ML method. Thus, using the DoE + ML method, we correlated the reaction conditions with the performance in organic light-emitting devices (OLEDs) and optimised the device performance by searching for the optimal reaction condition. As a result, the present study allowed us to optimise the performance of OLEDs, following some important principles of green and sustainable chemistry.[5]

Results and discussion

DoE + ML method

Previously, we developed a method for the one-pot synthesis of [*n*]cyclo-*meta*-phenylenes ([*n*]CMPs) by adopting the Ni-mediated Yamamoto coupling reaction for macrocyclisation.[6,7] The method was used to synthesise unique nanocarbon molecules,[8,9] which also allowed us to develop multipotent OLED materials.[10] For example, using dihalotoluene (**1**) as a starting material, we

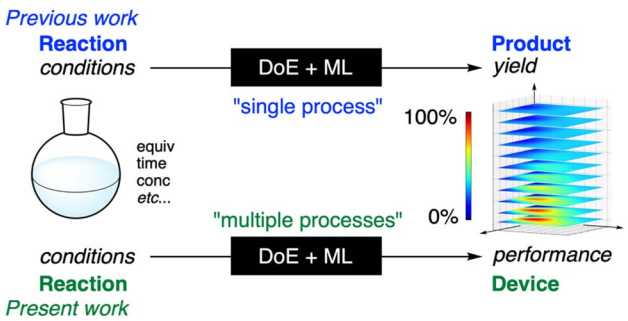

Fig. 1 "DoE + ML" method. Optimisation of reaction conditions traditionally correlates the conditions with the yields, but the present work demonstrates that the optimisation can correlate the reaction conditions with the performances of organic devices obtained through multistep processes.

[a]*Department of Chemistry, The University of Tokyo, Hongo 7-3-1, Bunkyo-ku, Tokyo 113-0033, Japan. E-mail: kikemoto@chem.s.u-tokyo.ac.jp; isobe@chem.s.u-tokyo.ac.jp*

[b]*Konica Minolta, Ishikawacho 2970, Hachioji, Tokyo 192-8505, Japan*

† Electronic supplementary information (ESI) available. See DOI: https://doi.org/10.1039/d4sc07039a

‡ K. Ikemoto and M. Akiyoshi have equally contributed to this work.

synthesised a series of [*n*]CMPs to fabricate single-layer OLEDs doped with Ir emitters (Fig. 2a).[10a] The highest performance of external quantum yield (EQE) = 22.8% was achieved with the methylated [5]CMP congener, while the performance of other congeners was inferior.[11] Considering the growing importance of developing low-cost, energy-saving and environmentally benign OLEDs for low-end consumables, we envisioned that the [*n*]CMP-based OLEDs can provide an interesting test case for development. Thus, the Yamamoto macrocyclisation afforded a series of [*n*]CMP congeners from $n \geq 5$ (*cf.* Fig. 2a for a MALDI mass spectrum) without any other noticeable byproducts, and, albeit with a range of EQE performance, the methylated [*n*]CMP derivatives generally acted as host materials for the Ir emitter.[10a] Therefore, we reasoned that we could directly use the crude raw material from the reaction for the Ir-doped OLEDs, skip energy-consuming and waste-producing processes such as separation and purification and thus optimise the conditions of the macrocyclisation reaction for the high-performance devices with the DoE + ML method (Fig. 2b).

Our DoE + ML method starts by deciding factors and levels for the optimisation to select an appropriate table from Taguchi's orthogonal arrays.[3,4] Three factors, *i.e.*, equivalent of $Ni(cod)_2$ (*M*), dropwise addition time of **1** (*T*) and final concentration of **1** (*C*), which were previously found to be influential in Yamamoto macrocyclisation, were also adopted in this study,[4,12] and additional two factors, *i.e.*, % content of bromochlorotoluene (**1b**) in **1** (*R*) and % content of DMF in solvent (*S*), were adopted to tweak the product distribution by changing the kinetics at the oxidative addition step and the disproportionation step, respectively.[6] Since we decided to examine three levels for each factor, there were 5 factors and 3 levels for the optimisation, and the DoE parameter space was set by referring to the "L_{18} ($2^1 \times 3^7$)" table of Taguchi's orthogonal arrays (Fig. 3a).[3] Among the 8 × 18 cells of the L_{18} ($2^1 \times 3^7$) table, 5 × 18 cells were selected to cover the 5 factors, and the 3 levels for each factor were set as shown in Fig. 3a to complete the experimental design. We carried out the 18

(a) L_{18} ($2^1 \times 3^7$)

	1	2	3	4	5	6	7	8
1	1	1	1	1	1	1	1	1
2	1	1	2	2	2	2	2	2
3	1	1	3	3	3	3	3	3
4	1	2	1	1	2	2	3	3
5	1	2	2	2	3	3	1	1
6	1	2	3	3	1	1	2	2
7	1	3	1	2	1	3	2	3
8	1	3	2	3	2	1	3	1
9	1	3	3	1	3	2	1	2
10	2	1	1	3	3	2	2	1
11	2	1	2	1	1	3	3	2
12	2	1	3	2	2	1	1	3
13	2	2	1	2	3	1	3	2
14	2	2	2	3	1	2	1	3
15	2	2	3	1	2	3	2	1
16	2	3	1	3	2	3	2	2
17	2	3	2	1	3	1	3	3
18	2	3	3	2	1	2	1	1

3 levels *M* (eq.): 2, 5, 10
T (min): 1, 5, 20
C (mM): 1, 10, 40
R (%): 0, 50, 100
S (%): 17, 50, 83

(b)

(*M*,	*T*,	*C*,	*R*,	*S*)	EQE (%)
(2,	1,	1,	0,	17)	1.4 ± 0.0
(2,	5,	10,	50,	50)	2.4 ± 0.0
(2,	20,	40,	100,	83)	5.4 ± 0.1
(5,	1,	1,	50,	50)	2.3 ± 0.0
(5,	5,	10,	100,	83)	3.0 ± 0.0
(5,	20,	40,	0,	17)	8.9 ± 0.1
(10,	5,	1,	100,	17)	2.5 ± 0.6
(10,	20,	10,	0,	50)	2.7 ± 0.0
(10,	1,	40,	50,	83)	4.9 ± 0.0
(2,	20,	1,	50,	83)	1.6 ± 0.0
(2,	1,	10,	100,	17)	5.4 ± 0.0
(2,	5,	40,	0,	50)	8.4 ± 0.2
(5,	5,	1,	0,	83)	0.6 ± 0.2
(5,	20,	10,	50,	17)	4.9 ± 0.0
(5,	1,	40,	100,	50)	8.0 ± 0.1
(10,	20,	1,	100,	50)	4.4 ± 0.0
(10,	1,	10,	0,	83)	2.0 ± 0.0
(10,	5,	40,	50,	17)	5.3 ± 0.1

Fig. 3 DoE-guided experiments. (a) The "L_{18} ($2^1 \times 3^7$)" table of Taguchi's orthogonal arrays. (b) Reaction conditions and EQE data (experimental values), covering 18 parameter sets of the "L_{18} ($2^1 \times 3^7$)" table.

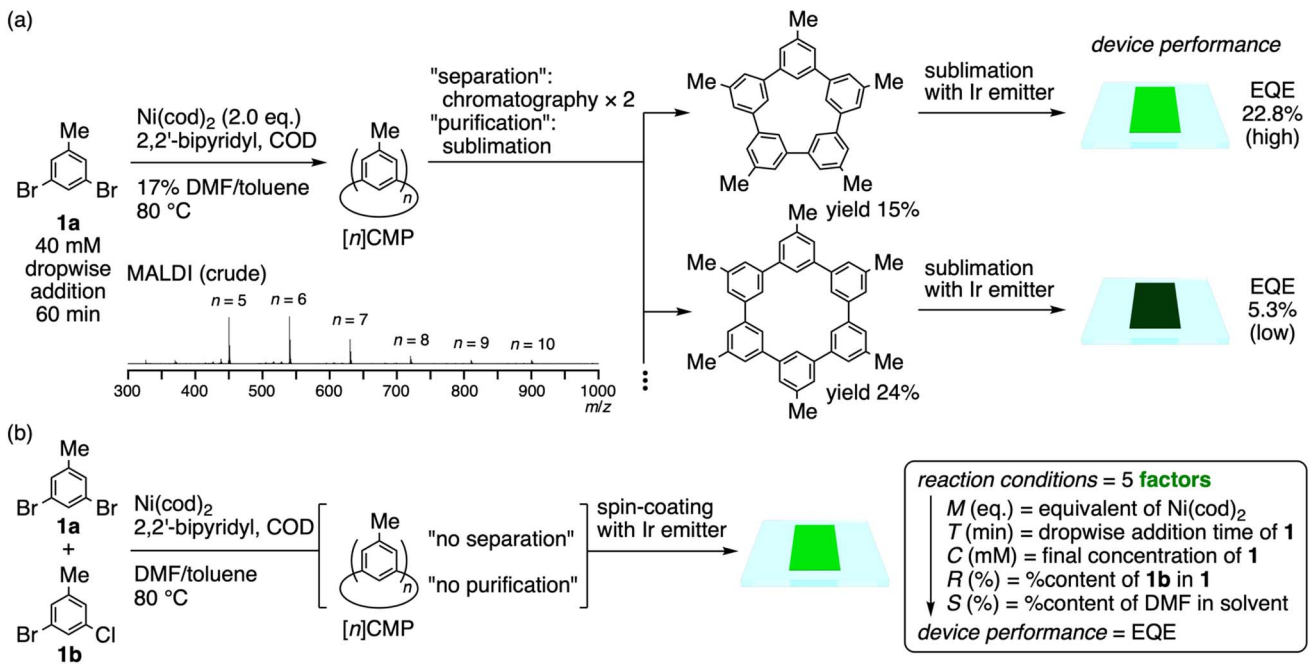

Fig. 2 Fabrication of [*n*]CMP-based OLEDs. (a) Multistep, stepwise processes used in traditional device fabrication protocols.[10a] (b) Simplified multistep processes used in the present study, which eliminated energy-consuming and waste-producing separation and purification steps.

reactions of Yamamoto macrocyclisation of **1** under the designed conditions, and 18 sets of crude raw materials were obtained after aqueous workup and passing the mixture through a short-path silica gel column to remove metal and polar residues (see ESI† for details).

The device performance of each of the 18 raw materials was evaluated by fabricating double-layer OLEDs, which was further supplemented by ML predictions.[13] Thus, the double-layer OLED was fabricated by first spin-coating a solution of a crude raw mixture of methylated [*n*]CMPs mixed with the Ir emitter (**3**; 14 wt% in the layer)[14] as the emission layer (EML; 20 nm) and then sublimating 1,3,5-tris(1-phenyl-1*H*-benzimidazol-2-yl)benzene (TPBi, **2**) as the overlaid electron transport layer (ETL; 60 nm) (*cf.* Fig. 4b). The device performance was evaluated by EQE in quadruplicate to correlate the five reaction factors of (*M*, *T*, *C*, *R*, *S*) with the EQE performance (Fig. 3b). For the ML predictions based on the EQE data, we investigated three ML methods, *i.e.*, support vector regression (SVR), partial least squares regression (PLSR) and multilayer perceptron (MLP), to obtain the EQE heatmaps to fill the five-dimensional parameter space of (*M*, *T*, *C*, *R*, *S*) (Fig. S6†).[4] As representative heatmaps, the (*M*, *T*, *C*) heatmaps at (*R*, *S*) = (50, 50) are shown in Fig. 4a. The ML predictions of the three methods were then evaluated by the mean square errors (MSE) obtained *via* leave-one-out cross-validations (LOOCV)[15,16] to decide the SVR model as the most appropriate predictor (MSE: SVR = 0.0368, PLSR = 0.0396, MLP = 0.2606). Finally, the SVR model was validated by running two test runs (Fig. 4b). The grid search of the five-dimensional SVR model found the highest EQE spot of 11.3% at (*M*, *T*, *C*, *R*, *S*) = (2, 9, 64, 5, 33), and the actual test run at this spot yielded a comparable EQE value of 9.6 ± 0.1%. Another high EQE spot at (2, 11, 50, 8, 29) was arbitrarily selected to record the experimental EQE value of 9.3 ± 0.0%, which also agreed well with 10.2% of the SVR model. The results confirmed that the SVR model, which successfully correlated the reaction conditions with the device performance, was credible.

An advantage of the raw-material OLEDs was found by comparing the EQE performance with that of the pure-material OLEDs. When the double-layer OLED was fabricated using the methylated [*n*]CMP congener after separation and purification as a single compound, the device performance was much inferior to record EQE = 0.9 ± 0.1% and 0.8 ± 0.3% with *n* = 5 and 6, respectively (Fig. 4b). As found with the single-layer OLEDs using methylated [*n*]CMPs,[12] the device performance is dramatically affected by the well-ordered packing of the host molecules, and the pure-material OLED would be affected by the crystalline character facilitated by the spin-coating process. On the other hand, the raw material is composed of a mixture of the methylated congeners and should maintain the amorphous character to retain the performance as a host material even through the solution process of the spin coating. When we analysed the "hit" raw material obtained at (*M*, *T*, *C*, *R*, *S*) = (2, 9, 64, 5, 33), the population of methylated [*n*]CMP congeners were found as *n* = 5: 19%, *n* = 6: 26%, *n* = 7: 18%, *n* = 8: 8%, *n* = 9: 11%, *n* = 10: 5%, *n* = 11: 5%, *n* = 12: 4%, *n* = 13: 2%, *n* = 14: 1% and *n* = 15: 0.4% by using the signal intensities of the MALDI spectrum (Fig. S3†).[17] Formulation of such an elaborate mixture

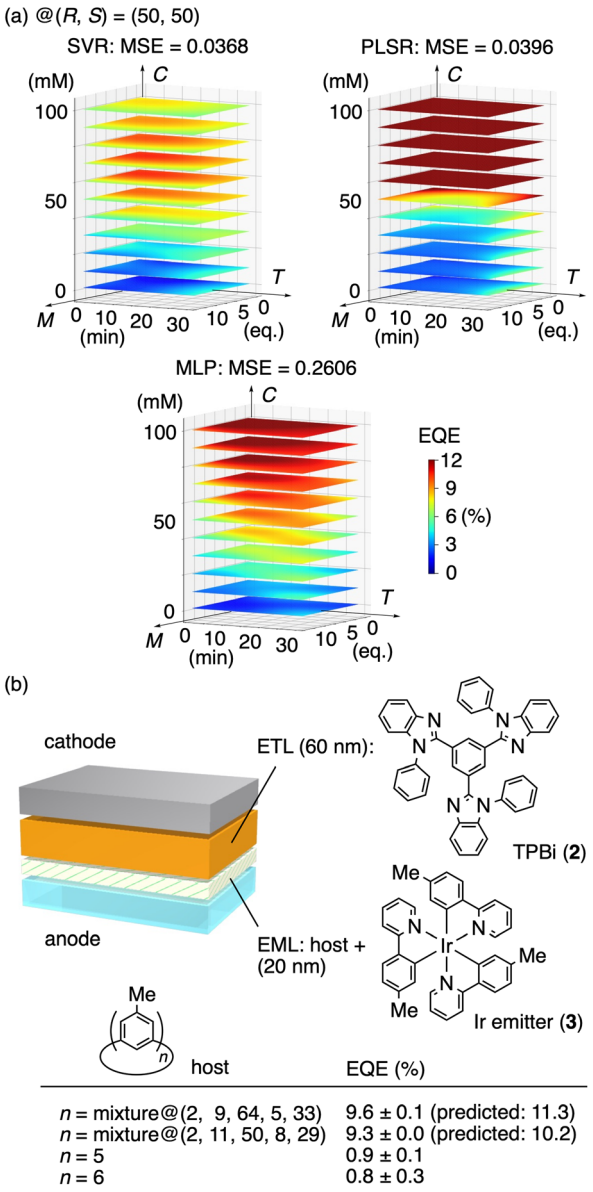

Fig. 4 Performance of raw-material OLEDs with [*n*]CMPs. (a) ML-derived heatmaps in the (*M*, *T*, *C*) parameter space at (*R*, *S*) = (50, 50). Three ML methods (SVR, PLSR, MLP) were evaluated with MSE to assign the SVR model as the best model. (b) Test runs to validate the SVR model with reference data using pure materials in the identical settings of OLEDs. A double-layer device architecture is also shown with molecular structures of the materials. Device architecture: cathode = LiF (2 nm)/Al (100 nm), ETL = **2** (60 nm), EML = 14 wt% **3** in a host material (20 nm), anode = PEDOT:PSS (60 nm)/ITO (120 nm).

of the [*n*]CMP congeners after standard separation/purification processes should not be easy,[18] which was succinctly achieved by a one-pot reaction without purification *via* ML-assisted design of the raw mixture material. Additional datasets of the [*n*]CMP population were also obtained by MALDI analysis of the raw materials from other (*M*, *T*, *C*, *R*, *S*) coordinates (Fig. S2†), which showed that the EQE changes of the device were originated from subtle changes in the [*n*]CMP population. The NMR spectra of the raw materials were also obtained, which allowed

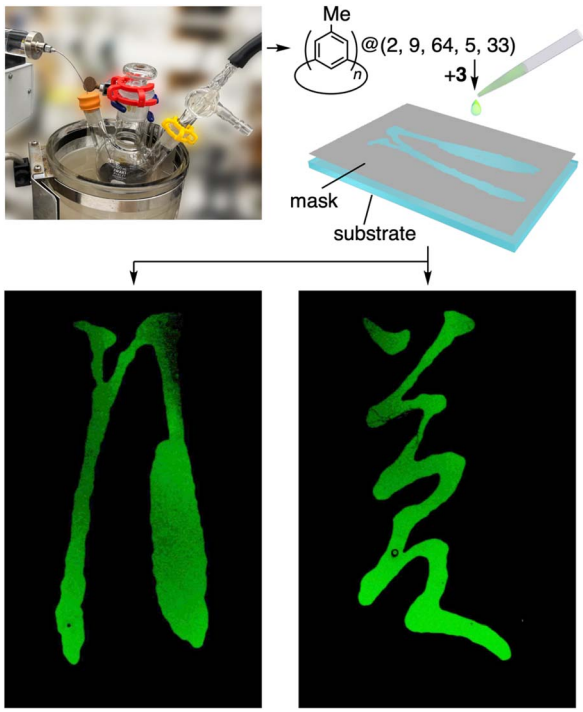

Fig. 5 Processes and images of screen-printed OLEDs using the raw-material mixture of methylated [*n*]CMPs from (*M*, *T*, *C*, *R*, *S*) = (2, 9, 64, 5, 33). The screen-printed images were created by copying kanji characters ((left): moon, (right): dream) written by a Japanese poet, Basho Matsuo.[20]

us to determine the yield of [*n*]CMP with $n = 5$, 6 and 7 by using an internal standard. The comparison of the MS and NMR populations of the congeners then confirmed (Fig. S4†), to a certain extent, that the MS population qualitatively reflected the [*n*]CMP population.

Screen-printed OLED

Finally, we applied the raw-material OLEDs *via* the flask-to-device processes to the screen-printing fabrication[19] (Fig. 5). Thus, the Yamamoto macrocyclisation of **1** was performed at the hit spot of (*M*, *T*, *C*, *R*, *S*) = (2, 9, 64, 5, 33) to afford the crude raw material consisting of the mixture of methylated [*n*]CMPs. The mixture was dissolved in chlorobenzene at 0.34 wt% together with 0.06 wt% of **3**. A glass coated with anode materials was covered with a metal mask bearing an image, and the EML solution was drop cast on the substrate. After removing the metal mask, the device was finished by coating with ETL (**2**; 60 nm) and cathode materials. The screen-printed device fabricated with raw-material [*n*]CMPs emitted light with images of kanji characters as shown in Fig. 5, demonstrating the applicability of the present strategy for the development of low-cost, environmentally benign OLEDs.

Conclusions

In summary, we have successfully demonstrated that the reaction conditions in the flask can be correlated with the performance in devices using the DoE + ML method. The crude, raw material from the reaction was found to be applicable as a host material in double-layer OLEDs, which succeeded in eliminating waste-producing, energy-consuming processes of separation and purification of small molecules. Although this "from-flask-to-device" optimisation strategy could not provide information on structure-performance relationships, the ML method provided a unique model that represented "reaction condition-performance relationships" in the five-dimensional parameter space. Importantly, the raw-material mixture was found to be superior to the pure material in terms of the device performance in the double-layer OLEDs, demonstrating the uniqueness and advantages of the "from-flask-to-device" strategy in generating elaborate mixture for materials. The development of small-molecule materials usually considers structure-performance relationships to a considerable extent, which indeed deepens our understanding of molecular materials,[21] but the direct connections made by the from-flask-to-device strategy with the help of growing ML technologies can also lead to the development of low-cost, environmentally benign organic devices in general. Design of a house-of-cards assembly of graphene-like molecules by using a mixture from the DoE + ML method, for instance, could be of interest to be applied for battery electrodes.[22]

Data availability

The data that support the findings of this study are available in the ESI.†

Author contributions

KI: conceptualization, data curation, formal analysis, funding acquisition, methodology, writing – original draft, writing – review & editing. MA: data curation, formal analysis, investigation, methodology, writing – original draft, writing – review & editing. AK: data curation, formal analysis, investigation. HK: data curation, formal analysis, investigation. HT: data curation, formal analysis, investigation. HI: conceptualization, data curation, formal analysis, funding acquisition, methodology, writing – original draft, writing – review & editing.

Conflicts of interest

There are no conflicts to declare.

Acknowledgements

H. I. thanks Professor Roald Hoffmann for sharing a draft manuscript of their stimulative, important essay before the publication (ref. 21), which was one of the important triggers for him to step forward in this unfamiliar field of machine learning. We thank undergraduate students who performed preliminary experiments at the early stage of this study during the May festival of the University of Tokyo. This work was partly supported by KAKENHI (20H05672, 22H02059) and A-STEP

(JPMJTR223C). M. A. thanks the JSPS and SPRING GX program for predoctoral fellowships.

Notes and references

1 C. Daniel, One-at-a-Time Plans, *J. Am. Stat. Assoc.*, 1973, **68**, 353–360.

2 C. K. Ingold, *Structure and Mechanism in Organic Chemistry*, Cornell University Press, Ithaka and London, 1969.

3 G. Taguchi, S. Chowdhury and Y. Wu, *Taguchi's Quality Engineering Handbook*, Wiley, Hoboken, 2005.

4 (*a*) K. Ikemoto, M. Akiyoshi, T. Mio, K. Nishioka, S. Sato and H. Isobe, Synthesis of a Negatively Curved Nanocarbon Molecule with an Octagonal Omphalos *via* Design-of-Experiments Optimizations Supplemented by Machine Learning, *Angew. Chem., Int. Ed.*, 2022, **61**, e202204035; (*b*) M. Akiyoshi, K. Ikemoto and H. Isobe, Tier-grown Expansion of Design-of-Experiments Parameter Spaces for Synthesis of a Nanometer-scale Macrocycle, *Chem.–Asian J.*, 2023, **18**, e202201141.

5 M. Doble and A. K. Kruthiventi, *Green Chemistry and Engineering*, Academic Press, Burlington 2007.

6 (*a*) T. Yamamoto, Y. Hayashi and A. Yamamoto, A Novel Type of Polycondensation Utilizing Transition Metal-Catalyzed C-C Coupling. I. Preparation of Thermostable Polyphenylene Type Polymers, *Bull. Chem. Soc. Jpn.*, 1978, **51**, 2091–2097; (*b*) T. Yamamoto, S. Wakabayashi and K. Osakada, Mechanism of C-C Coupling Reactions of Aromatic Halides, Promoted by Ni $(COD)_2$ in the Presence of 2,2'-Bipyridine and PPh_3, to Give Biaryls, *J. Organomet. Chem.*, 1992, **428**, 223–237.

7 (*a*) J. Y. Xue, K. Ikemoto, N. Takahashi, T. Izumi, H. Taka, H. Kita, S. Sato and H. Isobe, Cyclo-meta-phenylene Revisited: Nickel-Mediated Synthesis, Molecular Structures, and Device Applications, *J. Org. Chem.*, 2014, **79**, 9735–9739; (*b*) A. Yoshii, K. Ikemoto, T. Izumi, H. Taka, H. Kita, S. Sato and H. Isobe, Periphery Design of Macrocyclic Materials for Organic Light-Emitting Devices with a Blue Phosphorescent Emitter, *Org. Lett.*, 2019, **21**, 2759–2762.

8 (*a*) K. Ikemoto, T. M. Fukunaga and H. Isobe, Phenine Design for Nanocarbon Molecules, *Proc. Jpn. Acad., Ser. B*, 2022, **98**, 379–400; (*b*) K. Ikemoto, R. Kobayashi, S. Sato and H. and Isobe, Synthesis and Bowl-in-Bowl Assembly of a Geodesic Phenylene Bowl, *Angew. Chem., Int. Ed.*, 2017, **56**, 6511–6514; (*c*) K. Ikemoto, J. Lin, R. Kobayashi, S. Sato and H. and Isobe, Fluctuating Carbonaceous Networks with a Persistent Molecular Shape: A Saddle-Shaped Geodesic Framework of 1,3,5-Trisubstituted Benzene (Phenine), *Angew. Chem., Int. Ed.*, 2018, **57**, 8555–8559; (*d*) T. Mio, K. Ikemoto, S. Sato and H. Isobe, Synthesis of a Hemispherical Geodesic Phenine Framework by a Polygon Assembling Strategy, *Angew. Chem., Int. Ed.*, 2020, **59**, 6567–6571.

9 (*a*) U. Beser, M. Kastler, A. Maghsoumi, M. Wagner, C. Castiglioni, M. Tommasini, A. Narita, X. Feng and K. Müllen, A C216-Nanographene Molecule with Defined Cavity as Extended Coronoid, *J. Am. Chem. Soc.*, 2016, **138**, 4322–4325; (*b*) H. Hou, X.-J. Zhao, C. Tang, Y.-Y. Ju, Z. Y. Deng, X.-R. Wang, L.-B. Feng, D.-H. Lin, X. Hou, A. Narita, K. Müllen and Y.-Z. Tan, Synthesis and Assembly of Extended Quintulene, *Nat. Commun.*, 2020, **11**, 3976; (*c*) S.-H. Liu, H. Hou, Z.-Y. Deng, X.-R. Wang, C. Tang, Y.-Y. Ju, L.-B. Feng and Y.-Z. Tan, Three-Dimensional Conjugated Macrocycle with Large Polyaromatic Blocks Constructed by Post-π-Extension, *Sci. China:Chem.*, 2020, **63**, 1626–1631; (*d*) X.-J. Zhao, H. Hou, P.-P. Ding, Z.-Y. Deng, Y.-Y. Ju, S.-H. Liu, Y.-M. Liu, C. Tang, L.-B. Feng and Y.-Z. Tan, Molecular Defect-Containing Bilayer Graphene Exhibiting Brightened Luminescence, *Sci. Adv.*, 2020, **6**, 8541–8569.

10 (*a*) J. Y. Xue, T. Izumi, A. Yoshii, K. Ikemoto, T. Koretsune, R. Akashi, R. Arita, H. Taka, H. Kita, S. Sota and H. Isobe, Aromatic Hydrocarbon Macrocycles for Highly Efficient Organic Light-Emitting Devices with Single-Layer Architectures, *Chem. Sci.*, 2016, **7**, 896–904; (*b*) K. Ikemoto, A. Yoshii, T. Izumi, H. Taka, H. Kita, J. Y. Xue, R. Kobayashi, S. Sato and H. Isobe, Modular Synthesis of Aromatic Hydrocarbon Macrocycles for Simplified, Single-Layer Organic Light-Emitting Devices, *J. Org. Chem.*, 2016, **81**, 662–666; (*c*) T. Izumi, Y. Tian, K. Ikemoto, A. Yoshii, T. Koretsune, R. Arita, H. Kita, H. Taka, S. Sato and H. Isobe, Efficient Blue Electroluminescence from a Single-layer Organic Device Composed Solely of Hydrocarbons, *Chem.–Asian J.*, 2017, **12**, 730–733; (*d*) A. Yoshii, Y. Onaka, K. Ikemoto, T. Izumi, S. Sato, H. Kita, H. Taka and H. Isobe, Acyclic, Linear Oligo-meta-phenylenes as Multipotent Base Materials for Highly Efficient Single-layer Organic Light-emitting Devices, *Chem.–Asian J.*, 2020, **15**, 2181–2186.

11 With internal quantum efficiency (IQE) of 100%, OLED can achieve EQE of 20–30%, as a part of emitted light is confined within the device. See also ref. 10a.

12 The three factors, (*M*, *T*, *C*), were chosen, as we believed that these could be important factors that could influence intramolecular cyclization and intermolecular oligomerization. See also ref. 4a.

13 Our initial attempts to fabricate single-layer OLEDs by the spin-coating method were not successful (ref. 10a), as the method could not achieve necessary thickness to avoid the current leakage.

14 K. Dedeian, P. I. Djurovich, F. O. Garces, G. Carlson and R. J. Watts, A New Synthetic Route to the Preparation of a Series of Strong Photoreducing Agents: *fac* Tris-Ortho-Metalated Complexes of Iridium(III) with Substituted 2-Phenylpyridines, *Inorg. Chem.*, 1991, **30**, 1685–1687.

15 (*a*) A. C. Müller and S. Guido, *Introduction to Machine Learning with Python*, O'Reilly, Sebastopol, 2017; (*b*) D. M. Hawkins, S. C. Basak and D. Mills, Assessing Model Fit by Cross-Validation, *J. Chem. Inf. Comput. Sci.*, 2003, **43**, 579–586.

16 Z.-H. Zhou, *Machine Learning*, Springer, Singapore, 2021.

17 Careful examination of the isotope distributions of MALDI MS peaks showed that *n*-mer linear oligo-*meta*-phenylenes, [*n*]LOMP, were not included to any significant extent,

although [*n*]LOMP could also serve as the host. See also ref. 10d.

18 In previous studies, an elaborate mixture of small molecules was manually formulated for devices, which also requires another set of optimizations besides the reaction conditions. For example, see:(*a*) Y. Hino, H. Kajii and Y. Ohmori, Efficient Low-Molecule Phosphorescent Organic Light-Emitting Diodes Fabricated by Wet-Processing, *Org. Electron.*, 2004, **5**, 265–270; (*b*) M. Cai, T. Xiao, E. Hellerich, Y. Chen, R. Shinar and J. Shinar, High-Efficiency Solution-Processed Small Molecule Electrophosphorescent Organic Light-Emitting Diodes, *Adv. Mater.*, 2011, **23**, 3590–3596; (*c*) T.-H. Han, M.-R. Choi, C.-W. Jeon, Y.-H. Kim, S.-K. Kwon and T.-W. Lee, Ultrahigh-Efficiency Solution-Processed Simplified Small-Molecule Organic Light-Emitting Diodes Using Universal Host Materials, *Sci. Adv.*, 2016, **2**, e1601428; (*d*) R. Kumaresan, A. Maheshwaran, H.-Y. Park, K. Sung, J. Choi, W. Cho, M. Song, S. I. Ahn and S.-H. Jin, Non-Halogenated Solvent-Processed Highly Efficient Green Ir(III) Complexes with an External Quantum Efficiency Exceeding 23% for Phosphorescent Organic Light-Emitting Diodes, *J. Mater. Chem. C*, 2020, **8**, 12959–12967.

19 D. A. Pardo, G. E. Jabbour and N. Peyghambarian, Application of Screen Printing in the Fabrication of Organic Light-Emitting Devices, *Adv. Mater.*, 2000, **12**, 1249–1252.

20 B. Matsuo, *The Narrow Road to the Deep North (Oku no Hosomichi)*, Handwritten, Iwanami, Tokyo, 1997.

21 This study should also stimulate our discussion related to the phrase, "To predict is not to explain". See(*a*) R. Hoffmann and J.-P. Malrieu, Simulation *vs*. Understanding: A Tension, in Quantum Chemistry and Beyond. Part A. Stage Setting, *Angew. Chem., Int. Ed.*, 2020, **59**, 12590–12610; (*b*) R. Hoffmann and J.-P. Malrieu, Simulation *vs*. Understanding: A Tension, in Quantum Chemistry and Beyond. Part B. The March of Simulation, for Better or Worse, *Angew. Chem., Int. Ed.*, 2020, **59**, 13156–13178; (*c*) R. Hoffmann and J.-P. Malrieu, Simulation *vs.* Understanding: A Tension, in Quantum Chemistry and Beyond. Part C. Toward Consilience, *Angew. Chem., Int. Ed.*, 2020, **59**, 13694–13710.

22 (*a*) S. Sato, A. Unemoto, T. Ikeda, S. Orimo and H. Isobe, Carbon-Rich Active Materials with Macrocyclic Nanochannels for High-Capacity Negative Electrodes in All-Solid-State Lithium Rechargeable Batteries, *Small*, 2016, **12**, 3381–3387; (*b*) N. A. Kaskhedikar and J. Maier, Lithium Storage in Carbon Nanostructures, *Adv. Mater.*, 2009, **21**, 2664–2680.